thin rods, is solved. The analysis yields a set of stability criteria involving the system parameters such as the body moments of inertia, the length and mass distribution of the elastic rods, the lowest natural frequencies of the rods, and the satellite spin velocity. The power of the method is illustrated by the relative ease with which closed-form stability criteria are derived and by the amount of information which can be extracted from their ready physical interpretation. In particular, the analysis shows that, for stability, the spinning motion is to be imparted about the axis of maximum moment of inertia. This is the well-known "greatest moment of inertia" requirement. Moreover, the initial spin velocity Ω_c should not be merely lower than the first natural frequencies Λ_{1u} and Λ_{1v} associated with the transverse vibration of the rods (as the frequency of simple harmonic excitation of the rods should be if resonance is to be prevented), but the ratios Ω_s/Λ_{1u} and Ω_s/Λ_{1v} are dictated by the system parameters. Of course, for very stiff rods the natural frequencies Λ_{1u} and Λ_{1v} may be sufficiently high that the satisfaction of criteria (40) is ensured.

References

[1] Meirovitch, L., *Methods of Analytical Dynamics*, McGraw-Hill, New York, 1970.

[2] Pringle, R., Jr., "Stability of the Force-Free Motions of a Dual-Spin Spacecraft," *AIAA Journal*, Vol. 7, No. 6, June 1969, pp. 1054–1063.

[3] Likins, P. W. and Roberson, R. E., "Matrix Method for the Liapunov Stability Analysis of Cyclic Discrete Mechanical Systems," *Celestial Mechanics Journal*, to be published.

[4] Nelson, H. D. and Meirovitch, L., "Stability of a Nonsymmetrical Satellite with Elastically Connected Moving Parts," *The Journal of the Astronautical Sciences*, Vol. 13, No. 6, Nov.-Dec. 1966, pp. 226–234.

[5] Meirovitch, L. and Nelson, H. D., "On the High-Spin Motion of a Satellite Containing Elastic Parts," *Journal of Spacecraft and Rockets*, Vol. 3, No. 11, Nov. 1966, pp. 1597–1602.

[6] Meirovitch, L., "Stability of a Spinning Body Containing Elastic Parts via Liapunov's Direct Method," *AIAA Journal*, Vol. 8, No. 7, July 1970, pp. 1193–1200.

SEPTEMBER 1971 AIAA JOURNAL VOL. 9, NO. 9

Buckling of a Thin Annular Plate under Uniform Compression

SAURINDRANATH MAJUMDAR*

AiResearch Manufacturing Company, Torrance, Calif.

The buckling of a circular annular plate with the outer edge clamped, the inner edge free, and loaded with uniform radial compressive force applied at the outside edge has been studied both theoretically and experimentally. Solution to the differential equation for buckling has been sought in the form $w = A_n(r)\cos n\theta$, $n = 0,1,2,\ldots$. The differential equation has been solved exactly for $n = 0$ and $n = 1$ and approximately for higher values of n as well as for $n = 0$ and $n = 1$. The solutions indicate that for small ratios of inner to outer radius the plate buckles into a radially symmetric mode. When the ratio of the inner to outer radius exceeds a certain value, the minimum buckling load corresponds to buckling modes with waves along the circumference. The number of waves depends on the ratio of the inner and the outer radii. Tests were carried out with thin aluminum plates, and the results corroborate the theoretical predictions.

Nomenclature

a = outer radius
b = inner radius
D = bending stiffness of the plate $= Eh^3/[12(1-\nu^2)]$
E = modulus of elasticity of the plate
h = thickness of plate
T = temperature rise above ambient
V = potential energy
w = transverse displacement perturbation
ν = Poisson's ratio
α_A, α_S = coefficient of thermal expansion of aluminum and steel, respectively
θ_c = theoretical rise of temperature above ambient for buckling
N_0 = radial compressive force at the outer edge
N_{0cr} = radial compressive force at the outer edge at buckling
N_r = radial stress resultant
N_θ = circumferential stress resultant
$N_{r\theta}$ = shear stress resultant
T_c = experimentally observed rise of temperature above ambient for buckling

Received November 23, 1970; revision received March 24, 1971.

* Stress and Vibration Engineer; currently Graduate Research Assistant, University of Illinois. Associate Member AIAA.

Introduction

THE elastic stability of a thin circular plate was studied first by Bryan[1] in 1891. He showed that the minimum buckling load for a circular plate without a central hole corresponds to a radially symmetric buckling mode. The buckling of a circular annular plate subjected to shearing forces distributed along the edges was first studied by Dean.[2] Since then, many researchers have investigated the buckling of a circular annular plate subjected to various loading conditions. Willers[3] considered the case of a plate subjected to bending moment caused by initial stresses. Some of these cases have been extended to plates with varying thickness.[4–7] The buckling of a thin circular annular plate subjected to equal compressive loadings at both the edges has been studied by Olsson,[8] Schubert,[9] and Yamaki.[10] Olsson and Schubert considered only radially symmetric buckling modes. Yamaki showed that, for some cases, a radially symmetric buckling mode does not correspond to the lowest buckling load.

The buckling of a circular annular plate clamped at the outer edge with the inner edge free and subjected to uniform radial compression at the outer edge was first studied by Meissner.[11] He assumed a radially symmetric buckling mode and obtained a relationship between the buckling load and the ratio between the inner and the outer radii.

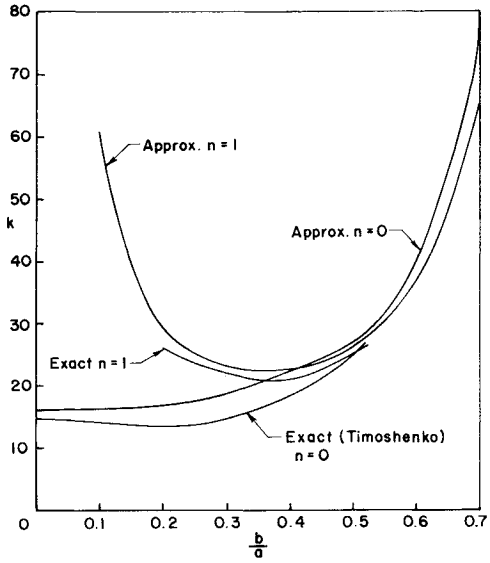

Fig. 1 Comparison between exact and approximate buckling loads.

The present paper considers the same problem but allows in the deflection pattern the possibility of various number of waves around the circumference. In particular, the differential equation of buckling for a single wave around the circumference has been solved exactly. Solutions for buckling with more than one wave around the circumference have been obtained using an approximate method. The results indicate that, if the ratio of the inner and the outer radii exceeds a certain minimum value, the radially symmetric buckling mode does not correspond to the lowest buckling load. The number of waves around the circumference which corresponds to the lowest buckling load, together with the lowest buckling load, increases with increasing ratios of the inner and the outer radii. Tests were conducted using thin aluminum plates, and the results corroborate the theoretical predictions.

Theory

The differential equation of buckling for a perfect circular annular plate of uniform thickness loaded radially at its edges is

$$D\nabla^4 w - N_r \frac{\partial^2 w}{\partial r^2} - N_\theta \left(\frac{1}{r}\frac{\partial w}{\partial r} + \frac{1}{r^2}\frac{\partial^2 w}{\partial \theta^2} \right) = 0 \qquad (1)$$

where

$$\nabla^4 = \nabla^2\nabla^2 = \left(\frac{\partial^2}{\partial r^2} + \frac{1}{r}\frac{\partial}{\partial r} + \frac{1}{r^2}\frac{\partial^2}{\partial \theta^2} \right) \times \left(\frac{\partial^2}{\partial r^2} + \frac{1}{r}\frac{\partial}{\partial r} + \frac{1}{r^2}\frac{\partial^2}{\partial \theta^2} \right)$$

and N_r and N_θ are the prebuckling membrane stresses.

For the case under consideration, the prebuckling membrane stresses are given by

$$\left.\begin{aligned} N_r &= -N_0 \frac{a^2}{a^2 - b^2}\left(1 - \frac{b^2}{r^2}\right) \\ N_\theta &= -N_0 \frac{a^2}{a^2 - b^2}\left(1 + \frac{b^2}{r^2}\right) \\ N_{r\theta} &= 0 \end{aligned}\right\} \qquad (2)$$

Substituting the expressions for N_r and N_θ from Eq. (2) into Eq. (1), the following equation is obtained:

$$\nabla^4 w + \lambda[(b^2)^{-1} + (r^2)^{-1}]\nabla^2 w = (2\lambda/r^2)(\partial^2 w/\partial r^2) \qquad (3)$$

where

$$\lambda = N_0 a^2 b^2 / D(a^2 - b^2)$$

The boundary conditions considered in the present case are

$$w = 0 \qquad \text{at } r = a \qquad (4)$$

$$\partial w/\partial r = 0 \qquad \text{at } r = a \qquad (5)$$

$$\frac{\partial^2 w}{\partial r^2} + \nu\left(\frac{1}{r}\frac{\partial w}{\partial r} + \frac{1}{r^2}\frac{\partial^2 w}{\partial \theta^2} \right) = 0 \qquad \text{at } r = b \qquad (6)$$

$$\frac{\partial}{\partial r}\left(\frac{\partial^2 w}{\partial r^2} + \frac{1}{r}\frac{\partial w}{\partial r} + \frac{1}{r^2}\frac{\partial^2 w}{\partial \theta^2} \right) + \frac{1-\nu}{r}\frac{\partial}{\partial \theta}\left(\frac{1}{r}\frac{\partial^2 w}{\partial r\,\partial \theta} - \frac{1}{r^2}\frac{\partial w}{\partial \theta} \right) = 0 \qquad \text{at } r = b \qquad (7)$$

Equations (3–7) pose an eigenvalue problem. The critical load obtained by solving these equations is usually expressed as

$$N_{0cr} = k(D/a^2) \qquad (8)$$

where k is related to the eigenvalue λ by the following equation:

$$k = \lambda[(a^2/b^2) - 1]$$

Solutions of Eq. (3) have been sought in the form

$$w = A_n(r)\cos n\theta \qquad \text{for } n = 0,1,2,\ldots \qquad (9)$$

Substituting the expression of w from Eq. (9) into Eq. (3) and using the transformation $Z = \lambda^{1/2}(r/b)$,

$$\frac{d^4 A_n}{dZ^4} + \frac{2}{Z}\frac{d^3 A_n}{dZ^3} - \left[\frac{1 + 2n^2 + \lambda}{Z^2} - 1 \right]\frac{d^2 A_n}{dZ^2} + \left[\frac{1 + 2n^2 + \lambda}{Z^3} + \frac{1}{Z} \right]\frac{dA_n}{dZ} + \left[\frac{n^2(n^2 - \lambda - 4)}{Z^4} - \frac{n^2}{Z^2} \right] \times A_n = 0 \qquad \text{for } n = 0,1,2,\ldots \qquad (10)$$

The case $n = 0$ corresponds to the radially symmetric buckling, and Eq. (10) reduces to

$$\frac{d^3\psi}{dZ^3} + \frac{2}{Z}\frac{d^2\psi}{dZ^2} + \left[1 - \frac{1+\lambda}{Z^2} \right]\frac{d\psi}{dZ} + \left[\frac{1+\lambda}{Z^3} + \frac{1}{Z} \right]\psi = 0 \qquad (11)$$

where $\psi = dA_0/dZ$. The three boundary conditions that Eq. (11) have to satisfy are Eqs. (5–7), which reduce to the following equations in terms of the variables ψ and Z:

$$\psi = 0 \qquad \text{at } Z = \lambda^{1/2}(a/b) \qquad (12)$$

$$(d\psi/dZ) + (\nu/Z)\psi = 0 \qquad \text{at } Z = \lambda^{1/2} \qquad (13)$$

$$(d/dZ)[(d\psi/dZ) + Z^{-1}\psi] = 0 \qquad \text{at } Z = \lambda^{1/2} \qquad (14)$$

A solution of Eq. (11) satisfying boundary condition (14) is

$$\psi = AJ_p(Z) + BJ_{-p}(Z) \qquad (15)$$

where $p = (\lambda + 1)^{1/2}$, $J_p(Z)$ and $J_{-p}(Z)$ are Bessels functions of the first kind, and A and B are arbitrary constants.

The imposition of boundary conditions (12) and (13) yield the following determinental equation for λ:

$$\begin{vmatrix} J_p\left(\lambda^{1/2}\frac{a}{b}\right) & J_{-p}\left(\lambda^{1/2}\frac{a}{b}\right) \\ J_{p-1}(\lambda^{1/2}) + \frac{\nu - p}{\lambda^{1/2}}J_p(\lambda^{1/2}) & J_{-p-1}(\lambda^{1/2}) + \frac{\nu + p}{\lambda^{1/2}}J_{-p}(\lambda^{1/2}) \end{vmatrix} = 0$$

A plot of the result is given by Timoshenko[12] and is reproduced in Fig. 1.

For the case $n = 1$ involving one wave around the circumference, Eq. (10) gives the following:

$$\frac{d^4A_1}{dZ^4} + \frac{2}{Z}\frac{d^3A_1}{dZ^3} + \left[1 - \frac{3+\lambda}{Z^2}\right]\frac{d^2A_1}{dZ^2} + \left[\frac{1}{Z} + \frac{3+\lambda}{Z^3}\right]\frac{dA_1}{dZ} - \left[\frac{1}{Z^2} + \frac{3+\lambda}{Z^4}\right]A_1 = 0 \quad (16)$$

Using the transformations $A_1 = Z\phi$ and $\psi = d\phi/dZ$, Eq. (16) can be reduced to

$$\frac{d^2\psi}{dZ^2} + \frac{3}{Z}\frac{d\psi}{dZ} + \left[1 + \frac{1-p^2}{Z^2}\right]\psi = \frac{C}{Z^3} \quad (17)$$

where $p^2 = \lambda + 4$ and C is an arbitrary constant. The general solution of Eq. (17) is

$$\psi = Z^{-1}[AJ_p(Z) + BJ_{-p}(Z) + CS_{-1,p}(Z)] \quad (18)$$

where

$$S_{-1,p}(Z) = \frac{\pi}{2\sin(p\pi)}\left[J_p(Z)\int\frac{J_{-p}(Z)}{Z}\times dZ - J_{-p}(Z)\int\frac{J_p(Z)}{Z}\,dZ\right]$$

and A,B are arbitrary constants. Writing $\psi(Z)$ in terms of $A_1(Z)$ in Eq. (18), the following is obtained:

$$Z(dA_1/dZ) - A_1 = Z[AJ_p(Z) + BJ_{-p}(Z) + CS_{-1,p}(Z)] \quad (19)$$

Boundary conditions (4–7), transformed into the new variables, can be written as

$$A_1 = 0 \qquad \text{at } Z = \lambda^{1/2}(a/b) \quad (20)$$

$$dA_1/dZ = 0 \qquad \text{at } Z = \lambda^{1/2}(a/b) \quad (21)$$

$$\frac{d^2A_1}{dZ^2} + \frac{\nu}{Z^2}\left[Z\frac{dA_1}{dZ} - A_1\right] = 0 \qquad \text{at } Z = \lambda^{1/2} \quad (22)$$

$$\frac{d^3A_1}{dZ^3} + \frac{1}{Z^2}\frac{d^2A_1}{dZ^2} - \frac{3-\nu}{Z^2}\frac{dA_1}{dZ} + \frac{3-\nu}{Z^3}A_1 = 0 \qquad \text{at } Z = \lambda^{1/2} \quad (23)$$

Subjecting the general solution (19) to the boundary conditions (20–23) leads to the following equations:

$$AJ_p[\lambda^{1/2}(a/b)] + BJ_{-p}[\lambda^{1/2}(a/b)] = 0 \quad (24)$$

$$A[(1+\nu-p)J_p(\lambda^{1/2}) + \lambda^{1/2}J_{p-1}(\lambda^{1/2})] + B[(1+\nu+p)J_{-p}(\lambda^{1/2}) + \lambda^{1/2}J_{-p-1}(\lambda^{1/2})] = 0 \quad (25)$$

$$C = 0 \quad (26)$$

For nontrivial solutions of A and B, the following equation must be satisfied:

$$\begin{vmatrix} J_p(\lambda^{1/2}\,a/b) & J_{-p}(\lambda^{1/2}\,a/b) \\ (1+\nu-p)J_p(\lambda^{1/2}) + \lambda^{1/2}J_{p-1}(\lambda^{1/2}) & (1+\nu+p)J_{-p}(\lambda^{1/2}) + \lambda^{1/2}\,J_{-p-1}(\lambda^{1/2}) \end{vmatrix} = 0$$

A plot of the results is shown in Fig. 1.

Approximate Solution

Solutions for cases involving $n > 1$ were obtained by the Rayleigh-Ritz method. A deflection pattern satisfying the displacement boundary conditions at the outer edge is

$$w = w_0[1 - (r^2/a^2)]^2\cos n\theta \qquad n = 0,1,2,\ldots \quad (27)$$

This expression for w was substituted in the expression for the total potential energy of the system given by

$$V = \frac{1}{2}\int_b^a\int_0^{2\pi}\left\{N_r\left(\frac{\partial w}{\partial r}\right)^2 + \frac{N_\theta}{r^2}\left(\frac{\partial w}{\partial\theta}\right)^2 + D\left[\left(\frac{\partial^2 w}{\partial r^2} + \frac{1}{r}\frac{\partial w}{\partial r} + \frac{1}{r^2}\frac{\partial^2 w}{\partial\theta^2}\right)^2 - 2(1-\nu)\frac{\partial^2 w}{\partial r^2}\left(\frac{1}{r}\frac{\partial w}{\partial r} + \frac{1}{r^2}\frac{\partial^2 w}{\partial\theta^2}\right) + 2(1-\nu)\left(\frac{1}{r}\frac{\partial^2 w}{\partial r\,\partial\theta} - \frac{1}{r^2}\frac{\partial w}{\partial\theta}\right)^2\right]\right\} r\,d\theta\,dr \quad (28)$$

where N_r and N_θ are given by Eq. (2). The total potential energy was then minimized with respect to w_0 to give the buckling load. A comparison between the exact and the approximate solutions for the two cases corresponding to $n = 0$ and $n = 1$ is shown in Fig. 1. In general, the difference between the exact and the approximate solutions are small. In the case of $n = 1$, the approximate solution gives exaggerated values of the buckling load for very small b/a ratios. The approximate solutions for higher values of n are shown in Fig. 2. The approximate solutions for $n > 1$ most likely provide exaggerated values of the buckling loads for very small b/a ratios. However, for values of b/a in this range, the lowest buckling load is given by $n = 0$. In order to determine whether the approximate solutions provide reasonable estimates of the minimum buckling loads for large b/a ratios, the following analogy is noted. An axially loaded long and narrow rectangular plate with one of its long edges clamped and the other edge free has a buckling load given by

$$N_{x_{cr}} = 13.1(D/d^2)$$

where d is the width of the plate. In the case of an annular plate, when b/a approaches unity, the compressed ring should behave like the plate just described. Hence, if a constant k' is defined for the annular plate such that

$$N_{\theta_{cr}}(r = a) = k'[D/(a-b)^2]$$

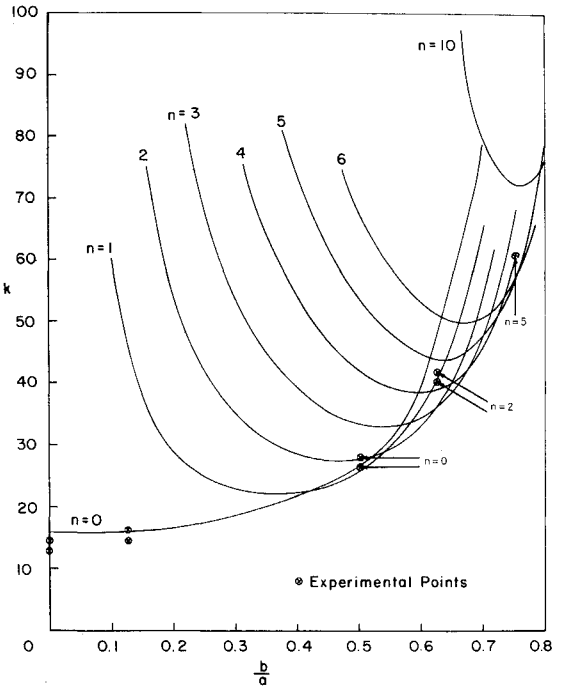

Fig. 2 Buckling load for various wave numbers.

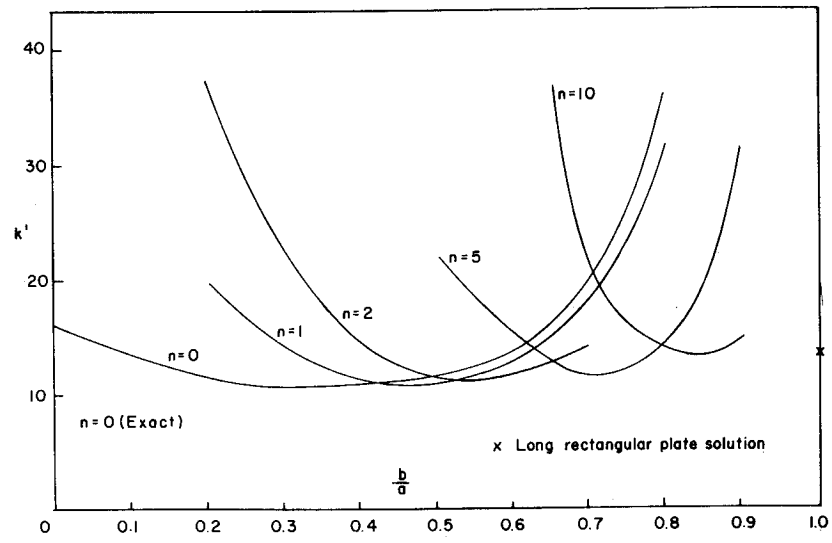

Fig. 3 Variation of modified buckling parameter k' with b/a.

then k' should approach a finite limit of 13.1 as b/a approaches unity. It can be shown that

$$k' = k[(a - b)/(a + b)][1 + (b^2/a^2)]$$

A plot of k' vs b/a for values of b/a up to 0.9 and with n as a parameter is shown in Fig. 3. It may be observed that the value of k' corresponding to the minimum buckling load varies very little throughout the entire range of b/a considered. The behavior of k' thus indicates that the one-term Rayleigh-Ritz procedure provides a reasonable estimate of the minimum buckling load for at least up to values of $b/a = 0.9$ and $n = 10$. It should be remembered, however, that for values of b infinitesimally close to a the assumptions of thin-plate theory are no longer valid, and the present analysis is incapable of handling such situations.

Test Results

Tests were carried out using 0.041-in.-thick 2024 aluminum plates clamped between two 0.5-in.-thick steel rings by means of 12 0.5-in. ϕ high tensile steel bolts, as shown in Fig. 4. The inner diameter of the steel ring was 8 in. and the outer diameter 10 in. The various plate geometries used in the tests are given in Table 1.

Loading was accomplished by heating the whole assembly, whereupon the steel rings put a uniformly distributed radial compressive load on the aluminum plate because of the difference in the coefficients of thermal expansion. The effects of the elasticity of the steel rings on the stress distribution in the plates and on the assumption of clamped edge condition were estimated to be very small.

The tests were carried out in two parts. Details of these tests may be obtained from Ref. 13.

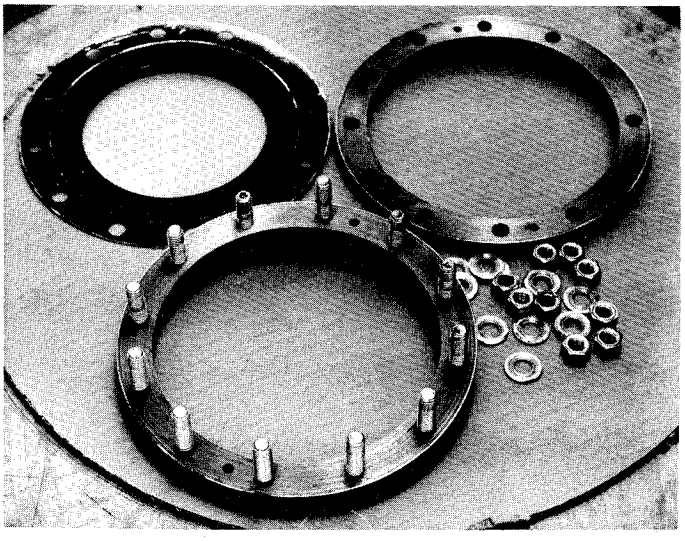

Fig. 4 Test specimen.

Test Series A

The assembly was heated inside a Missimers environment chamber, where the temperature of the specimens could be controlled to within $\pm 1°$F. To keep the temperature gradient in the specimen to a minimum, a soaking period of about 1 hr was allowed for each increment in temperature. Temperature-compensated radial and circumferential strain gages were attached on both sides of the plate. The difference in the strain gage readings on two sides of the plate gives a direct measure of the bending and consequently the transverse deflection of the plate. The plates start to bend from the beginning of loading because of the presence of initial imperfections. A Southwell type of plot was, therefore, used to obtain the buckling temperature T_c as shown in Fig. 5. θ_c in the figure represents the theoretically computed buckling temperature.

The buckling parameter k is related to the buckling temperature T_c by the following equations:

$$k = 12(1 + \nu)(a^2/h^2)[\alpha_A - \alpha_S]T_c \qquad \text{for solid plates}$$

$$k = 12(1 - \nu^2)\frac{a^2 - b^2}{a^2(1 - \nu) + b^2(1 + \nu)}\frac{a^2}{h^2}[\alpha_A - \alpha_S]\,T_c$$

for annular plates

The test points are shown in Fig. 2.

Test Series B

To obtain the number of waves along the circumference of the plates during buckling, a direct measurement of de-

Table 1 Geometry of test specimens

b, in.	b/a
0	0
0.5	0.125
2	0.5
2.5	0.625
3	0.75

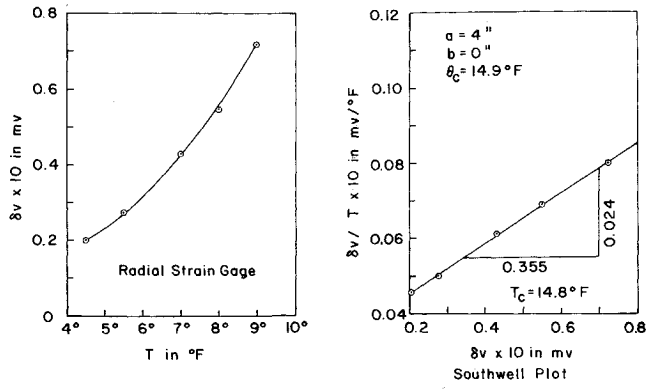

Fig. 5 Typical Southwell plot for obtaining buckling temperature.

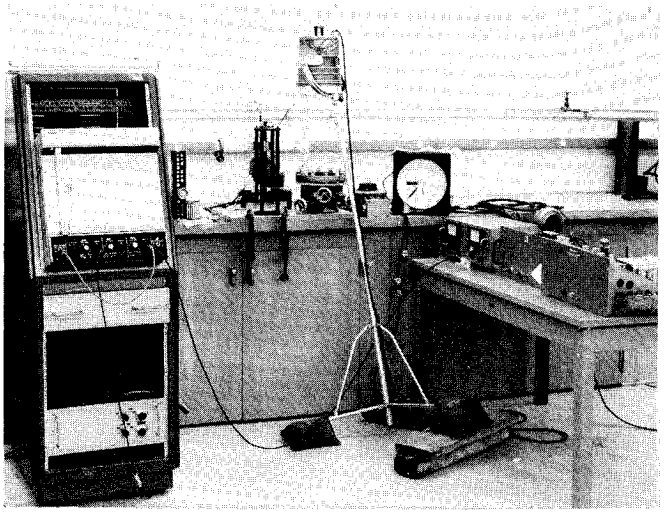

Fig. 6 Test setup for series B.

flection was made using an inductance pickup. The plate clamped by the rings was placed on a turntable that could be rotated, and the pickup was attached by means of an arm to a graduated optical bench (Fig. 6). The assembly was heated by means of a 1000-w quartz iodine photographic lamp connected in series with a rheostat. At every step of loading, the assembly was given enough time to reach equilibrium temperature. The plate was rotated with the pickup placed at a fixed radius, and the output from the pickup was plotted directly on an XY plotter. Even though the radial temperature distribution in the plate was somewhat nonl uniform, it affected only the mode shape along the radia-direction and did not alter the number of waves in the circumferential direction. Figures 7–11 show the circumferential variation of the deflection of various plates at a particular radius for each increment of loading.

Discussion

The test data (Fig. 2) in general indicate slightly higher buckling loads than the theoretically computed values. This is because a certain amount of slipping between the aluminum plate and the steel rings cannot be avoided, particularly at the higher buckling loads. As a result, the experimentally

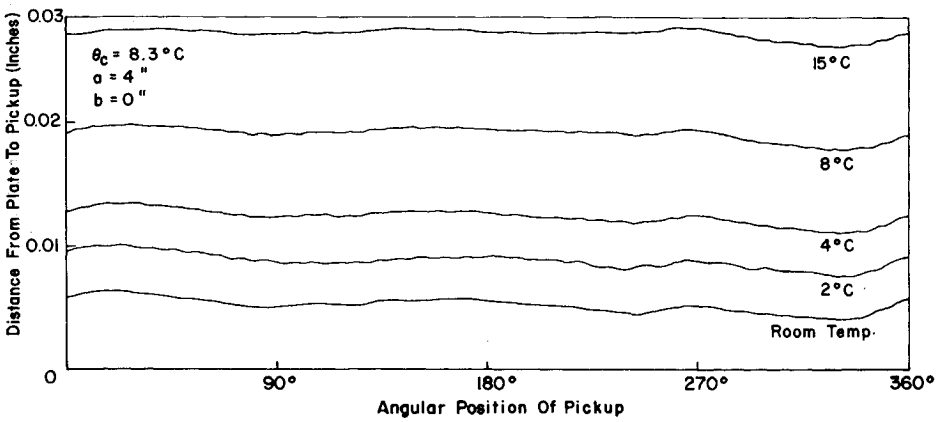

Fig. 7 Displacement at various circumferential stations with temperature.

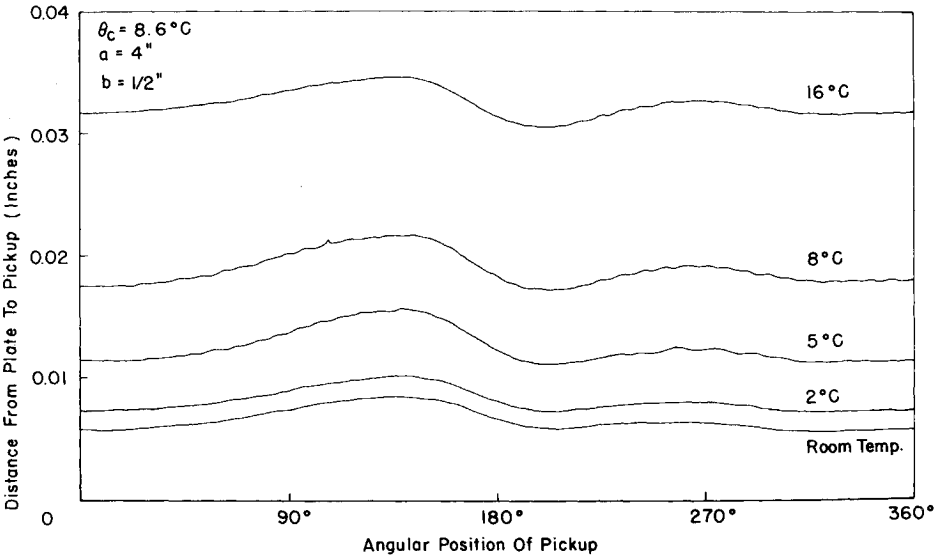

Fig. 8 Displacement at various circumferential stations with temperature.

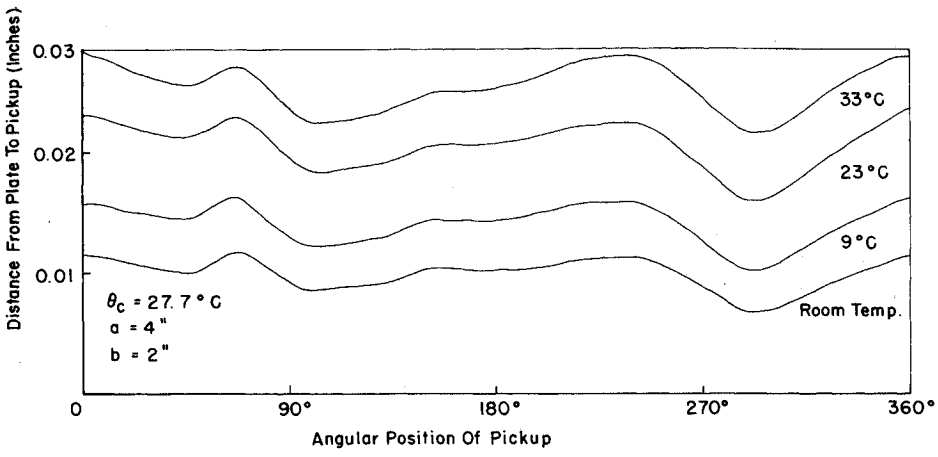

Fig. 9 Displacement at various circumferential stations with temperature.

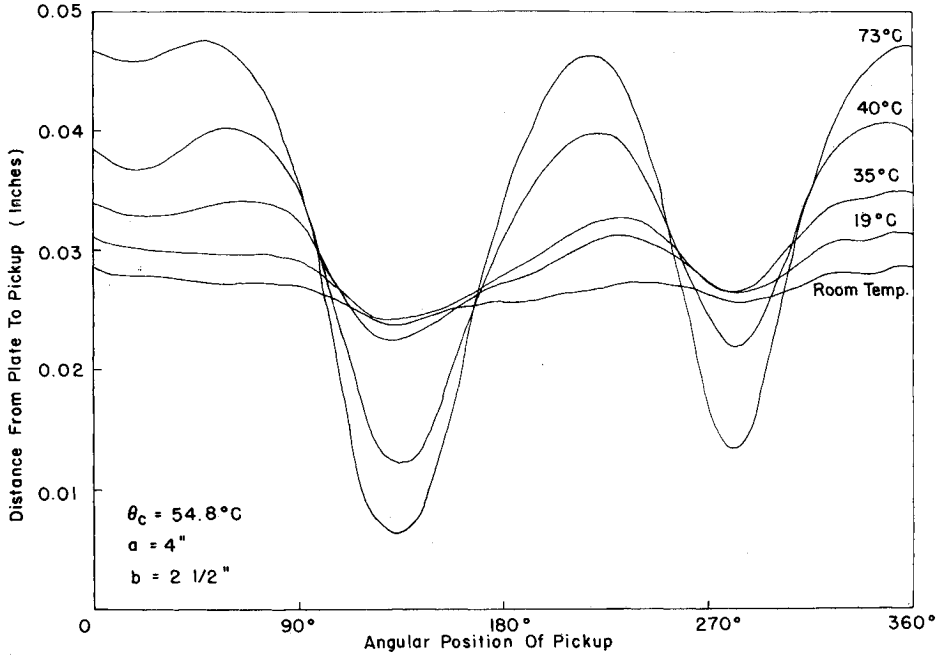

Fig. 10 Displacement at various circumferential stations with temperature.

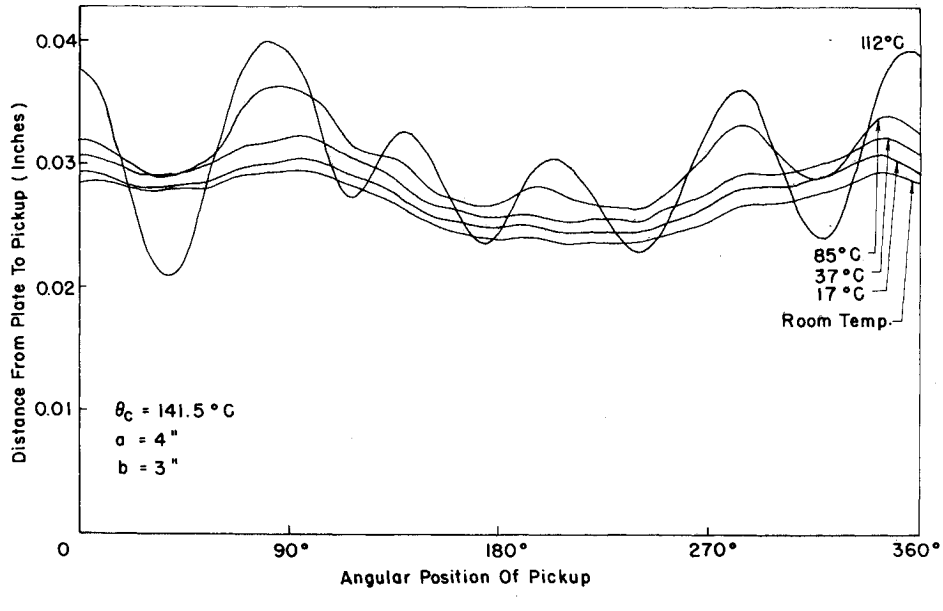

Fig. 11 Displacement at various circumferential stations with temperature.

observed buckling temperatures are slightly greater than what would be observed had there been no slipping.

The test data in general support the theoretical predictions. For small b/a ratios, the buckling mode observed is radially symmetric. For $b/a > 0.5$, the experimentally observed buckling modes contain waves around the circumference, and the number of waves and the buckling load increase with increasing b/a.

In each test, during the initial stages of loading the plate deforms in the primary mode of imperfection present, which is usually radially symmetric. As the load approaches the buckling value, however, the plate begins to develop circumferential waves, depending on the particular b/a ratio. This is to be expected, because the plate has a stable postbuckling behavior. For large b/a ratios, the buckling curves corresponding to various values of n tend to group together; as a result, the initial imperfection may influence the buckling mode.

It is interesting to compare the present case with the case 3 studied by Yamaki,[10] who analyzed a plate with similar displacement boundary conditions but loaded with equal pressure at both the boundaries. Yamaki showed that the minimum buckling load always occurs in a radially symmetric mode. The stress-free internal boundary condition thus changes the buckling behavior of the plate.

Conclusions

Experimental and theoretical work have been carried out on the problem of buckling of an annular plate subjected to uniform pressure on the clamped outer edge with the inner edge free. It has been shown that for this type of loading the buckling mode depends on the b/a ratio. This is in contrast to the situation where both the inner and the outer edges are subjected to equal pressure, in which case the buckling mode is radially symmetric for all b/a ratios.

The buckling stresses for different wave numbers are very close together for large b/a ratios. The mode in which the plate will buckle will, therefore, be influenced by the initial imperfections. However, since the plate has stable postbuckling behavior, the load at which the plate buckles will not be very sensitive to the initial imperfections.

References

[1] Bryan, G. H., "Buckling of Plates," *Proceedings of the London Mathematical Society*, Vol. 22, 1891, p. 54.

[2] Dean, W. R., "The Elastic Stability of an Annular Plate," *Proceedings of the Royal Society of London, England*, Ser. A, Vol. 106, 1924, p. 268.

[3] Willers, Fr. A., "Die Stabilitat von Kreisringplatten," *Zeitschrift fur angewandte Mathematik und Mechanik*, Vol. 23, 1943, p. 252.

[4] Federhofer, K. and Egger, H., "Knickung der auf Scherung beanspruchten Kreisringplatte mit veranderlicher Dicke," *Ingenieur-Archiv*, Vol. 14, 1943, p. 115.

[5] Federhofer, K., "Knickung der Kreisplatte und Kreisringplatte mit veranderlicher Dicke," *Ingenieur-Archiv*, Vol. 11, 1940, p. 224.

[6] Olsson, R. G., "Uber die Knickung der Kreisringplatte von veranderlicher Dicke," *Ingenieur-Archiv*, Vol. 12, 1941, p. 123.

[7] Egger, H., "Knickung der Kreisplatte und Kreisringplatte mit veranderlicher Dicke," *Ingenieur-Archiv*, Vol, 12, 1941, p. 190.

[8] Olsson, R. G., "Uber axialsymmetrische Knickung dunner Kreisringplatten," *Ingenieur-Archiv*, Vol. 8, 1937, p. 449.

[9] Schubert, A., "Die Beullast dunner Kreisringplatten, die am Aussen und Innenrand gleichmassigen Druck erfahren," *Zeitschrift fur angewandte Mathematik und Mechanik*, Vol. 25/27, 1947, p. 123.

[10] Yamaki, N., "Buckling of a Thin Annular Plate under Uniform Compression," *Report of the Institute of High Speed Mechanics, Sendai, Japan*, Vol. 10, 1959, pp. 129–147.

[11] Meissner, E., "Uber das Knicken kreisringformiger Scheiben," *Schweizerche Bauzeitung*, Vol. 101, 1933, p. 87.

[12] Timoshenko, S. and Gere, J. M., *Theory of Elastic Stability*, 2nd ed., McGraw-Hill, New York, 1961, p. 392.

[13] Majumdar, S., "Buckling of Thin Annular Plates due to Radial Compressive Loading," thesis submitted in partial fulfillment of the requirements for the degree of Aeronautical Engineer, 1968, California Institute of Technology, Pasadena, Calif.